Desalination and Water Treatment
www.deswater.com
doi: 10.1080/19443994.2013.794713

52 (2014) 2440–2449
March

Taylor & Francis
Taylor & Francis Group

Preparation of activated carbon derived from leather waste by H_3PO_4 activation and its application for basic fuchsin adsorption

Jiaojiao Kong, Lihui Huang*, Qinyan Yue, Baoyu Gao

Shandong Provincial Key Laboratory of Water Pollution Control and Resource Reuse, School of Environmental Science and Engineering, Shandong University, Jinan 250100, China
Tel. +86 531 88366873; Fax: +86 531 88364513; email: huanglihui9986@126.com

Received 5 February 2013; Accepted 6 April 2013

ABSTRACT

Leather activated carbon (LAC) was prepared from the leather waste by H_3PO_4 impregnated at 105°C for 3 h and activated at 450°C for 1 h in a muffle furnace. Based on LAC, Mn-modified leather activated carbon (LAC-Mn) was also studied. The two adsorbents were characterized by scanning electron microscopy, pore distribution, N_2 adsorption/desorption isotherms, Fourier transform infrared spectroscopy, and X-ray photoelectron spectroscopy. Several factors, such as contact time, dosage, and pH were studied, which indicated that cation exchange, hydrophobicity, and π-electron-donor–acceptor interaction were likely the adsorption mechanisms for basic fuchsin adsorption. Meanwhile, adsorbent effects of LAC and LAC-Mn were highly pH dependent, which reached maximum under alkaline conditions. The adsorption kinetic followed the pseudo-second-order kinetic model with high correlation coefficients ($R^2 > 0.99$), which means intra-particle diffusion process was not the only mechanism involved. Thermodynamics showed that the Langmuir isotherm equation can describe adsorption isotherms, and the maximum adsorption capacity of activated carbon increased from 139.28 to 182.48 mg/g after being modified by Mn(II). The adsorption process was a spontaneous and endothermic process.

Keywords: Adsorption; Basic fuchsin; Mechanism; Leather activated carbon; Modified by Mn(II)

1. Introduction

Dyes have been widely applied in many industries, such as printing, leather tanning, optical communication, etc. Thus, nowadays a large amount of dye wastewater is produced, which is not only toxic to all life-forms [1] but also badly affect the appearance of surface water. Basic fuchsin, a complex red phenyl methane dye, is often used in biological experiments as a biological stain, which is the most powerful nuclear dye and is also used in textile industry [2]. It is also applied as coloring agent in paper printing and textile dyeing.

Activated carbon is well known because of its highly developed porous structure and high adsorption capacity. However, its high cost limits the application of activated carbon in large-scale treatments. Nowadays, some researchers have searched for cheaper material as the precursor, including date pits [3], agricultural solid wastes [4], silk cotton hull [5], Indian Rosewood sawdust [6], oak sawdust [7], etc.

*Corresponding author.

To our knowledge, the main original material of preparing activated carbon is cellulose, and the activated carbon produced by protein is lighter than that produced by cellulose. Leather waste is one of the three waste streams in tanning industry, which has a certain amount of protein. The landfill of leather waste disposal would occupy a larger area of land, thus the eco-friendly treatment methods should be taken measures.

In this study, leather waste was used as the precursor to prepare activated carbon, which is also an economic method to deal with the solid waste. A few investigations have used leather waste as an activated carbon raw material [8]. H_3PO_4 and $MnSO_4$ were chosen as the activating and modifying agent, respectively. In the previous study, leather activated carbon (LAC) modified by Mn(II) was not discussed. The research aimed to compare the properties of original and modified activated carbons under different conditions, and discuss the adsorption mechanism. The surface physical and chemical properties of activated carbon were also characterized using the scanning electron microscopy (SEM), surface area analyzer, Fourier transform infrared spectroscopy (FTIR), and X-ray photoelectron spectroscopy (XPS).

2. Materials and methods

2.1. Materials

The start material used in the activated carbon was the leather waste in a tanning industry. The analogue dye wastewater was prepared with basic fuschin ($M_W = 337.85$, chemical formula $C_{20}H_{20}ClN_3$, and $\lambda_{max} = 543$ nm). The molecular structure of basic fuschin is illustrated in Fig. 1. All the reagents used were of analytical grade, and the experimental water was deionized water.

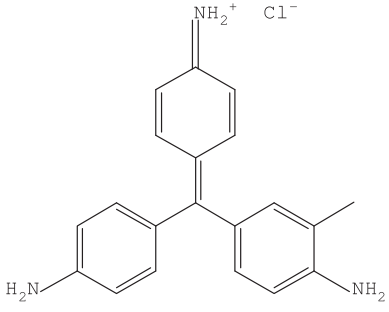

Fig. 1. The molecular structure of BF.

2.2. Preparation of LAC

LAC was prepared as follows: the leather waste was washed with the deionized water repeatedly to remove the dust, and then be heated at 50 ℃. The dried material was crashed into a number of particles with diameter of 5–10 mm by using a scissors, then was dipped with a 40 wt.% H_3PO_4 solution at a ratio of 1:1 (g L/g H_3PO_4) at 105 ℃ for 3 h. After that, the impregnated samples were placed into a pyrolysis reactor and activated at 450 ℃ for an hour in a muffle furnace. When the char cooled down to the room temperature, the sample was boiled with 40 ml of 10% HCl to nearly dry. Then, the mixture was washed with deionized water to remove the chloride ions and other ions until the pH of the filtrate reached neutral and heated at 120 ℃ for 2 h. Ultimately, the dried sample was crushed and sieved at the mesh size of 100–140 mesh, and kept in a desiccator for study. After the above process, the leather waste activated carbon (LAC) was acquired.

Modified leather waste activated carbon was prepared by the following steps: a certain amount of LAC was mixed with 100 ml $MnSO_4$ solution (100 mg/L), and then shook at 125 rpm in a water bath shaker for 24 h. Then, the solid was separated from the solution using the vacuum filtration, and heated at 105 ℃ for 12 h. Thus, the Mn-modified activated carbon was referred to as Mn-modified leather activated carbon (LAC-Mn).

2.3. Characterization of activated carbons

The surface morphology of activated carbons was measured by the SEM (Hitachi S-520, Japan). Aperture properties and Brunauer–Emmett–Teller (BET) surface areas of LAC and LAC-Mn were determined by a surface area analyzer (Quantachrome Corporation, USA), and N_2 as the adsorbate at 77 K. The specific surface areas (S_{BET}) and the total pore volume (V_t) were estimated from the manufacturer's software; the micropore surface area (S_{mic}), external surface area (S_{ext}), as well as the micropore volume (V_{mic}) were derived from *t*-plot method; the pore size distribution was deduced based on the density functional theory and the BET. From the relation: $D_p = 4V_t/S_{BET}$, the mean pore (D_p) can be determined. The surface functional groups of activated carbons were determined by FTIR (Fourier-380FTIR, USA). The element speciation and chemical oxidation state of Mn before and after adsorption were measured by XPS. It was determined using a spectrometer (ESCALAB 250) with Mg Kα irradiation (1,486.71 eV of photons) as an X-ray source.

2.4. Experiment

2.4.1. Adsorption experiments

Several influencing factors of BF adsorption on LAC and LAC-Mn were discussed, such as pH and adsorbent dose. For each experiment, a certain amount of LAC or LAC-Mn was added into a 250-mL Erlenmeyer flask containing 100 ml solution of basic fuchsin, and shaken at 20 ± 1℃ in a water bath shaker (SHZ-88) until the equilibrium was reached. Then the BF solution was filtered and the absorbance of the filtrate was determined by a UV/visible spectrophotometer (UV-754, shanghai, China) at the maximum wavelength (λ_{max} = 543 nm). In pH studies, the initial pH was regulated to 3–11 using different concentrations (0.01, 0.1, 1.0, and 2.0 M) of HCl or NaOH. The adsorption isotherm experiments were performed at 20, 30, and 40℃. The adsorption capacity (q_e (mg/g)) and percent removal of BF were calculated from the following equation:

$$q_e = \frac{(C_0 - C_e)V}{W} \quad (1)$$

$$\text{Removal } (\%) = \frac{C_0 - C_e}{C_e} \times 100 \quad (2)$$

where C_0 (mg/L) and C_e (mg/L) are the initial and equilibrium concentrations of BF solutions, respectively. V (L) is the volume of BF solutions and W (g) is the mass of activated carbon.

The adsorption kinetic experiment was carried out in a 1,000 ml beaker, which was placed on an electromagnetic stirrer at 20℃ with a speed of 125 rpm. A certain mass (1 g) LAC or LAC-Mn was added into 1,000 ml BF solution with the initial concentration of 150 mg/L. At a certain time interval, 10 ml sample was taken out and filtered to determine the concentration of filtrate. And the adsorption amount at a specific time, q_t, is determined by the following equation:

$$q_t = \frac{(C_0 - C_t)V}{W} \quad (3)$$

where q_t (mg/g) represent adsorption amount of BF at a particular time.

2.4.2. Desorption experiments

The distilled water or different concentrate NaOH solution (0.05, 0.1, 0.15, and 0.2 M) was used to conduct the desorption experiment. After the activated carbon was saturated with BF solution, the adsorbent was filtered and washed to remove the BF on the surface. Then, the sample was dried in a vacuum oven at 80℃. After that, a certain mass of activated carbon was mixed with 100 ml of distilled water or different concentrate NaOH solution, and agitated at 20 ± 1℃ for 24 h. And the percentage of desorption was determined using the following equation:

$$\%\ \text{Desorption} = \frac{m_d}{m_a} \quad (4)$$

where m_d (mg/L) is the amount of BF desorbed and m_a (mg/L) is the amount of BF adsorbed.

3. Results and discussion

3.1. Characterization of activated carbons

3.1.1. Analysis of SEM and pore structure

The surface structure property of LAC and LAC-Mn can be shown in Fig. 2. It was seen that the two adsorbents had a rough and loose surface, which was scattered with different size apertures. The reason can be explained that the raw material was dipped with phosphoric acid at high temperature could accelerate depolymerization, dehydration, and particle swelling of the protein material [9]. The shrink of pore was hindered in the process of activation due to the occupancy of phosphoric acid molecule, thus the developed pore structure formed. The pore structure was small, which can be explained that leather waste has low carbon content in mass than lignocelluloses material and form small pores. After modifying by Mn(II), the pores were diminished.

The pore size distribution and N_2 adsorption/desorption isotherms of LAC and LAC-Mn are shown in Fig. 3. The pore size distribution shows that most of the pores belonged to the micro-mesopores (<5 nm). According to the International Union of Pure and Applied Chemistry, this N_2 adsorption/desorption isotherms for both of the adsorbents corresponded with the IV curve. The surface areas and porosities of LAC and LAC-Mn are displayed in Table 1. It can be shown that the LAC-Mn had a high specific surface area (S_{BET}) than LAC, and the BET surface area increased by 14.34% and the total pore volume by 31.61%. The results could be explained that the sedimentation of Mn oxides as its oxidation process could enhance the development of micropore and increased the surface area of micropore. Thus, the BET surface area and total pores volume increased.

3.1.2. FTIR results

The surface functional groups which played important role in the properties of activated carbon

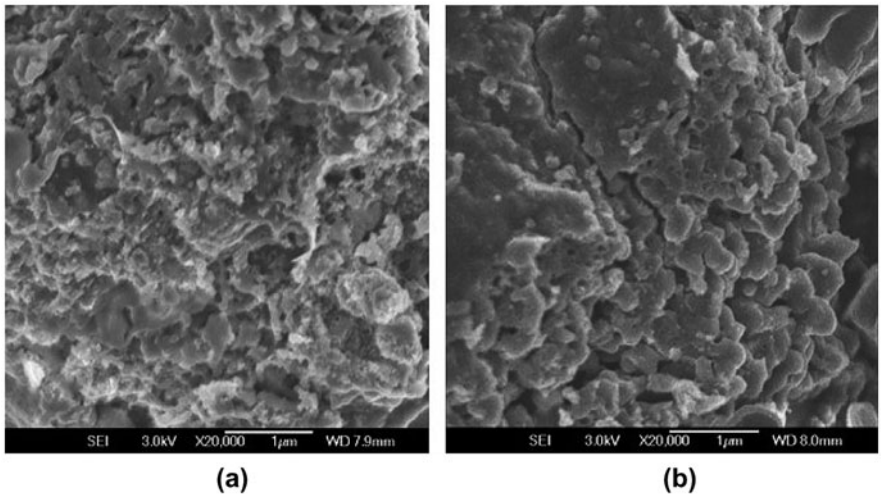

Fig. 2. Scanning electron micrograph of LAC (a) and LAC-Mn (b).

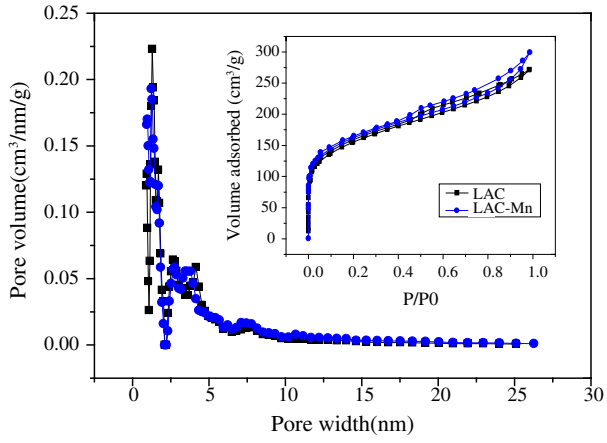

Fig. 3. Pore size distribution curves of the adsorbent and the insert figure is N_2 adsorption/desorption isotherms.

can be perceived from the infrared spectrum curves. It is shown in Fig. 4(a) that the peaks of LAC absorbance bands were at 502.42, 1,237.63, 1,414.33, 1,561.78, and 1,616.50 cm^{-1}, while the LAC-Mn at 507.31, 591.94, 751.87, 1,043.19, 1,232.65, 1,408.30, and 1,572.84 cm^{-1}. The peaks between 1,000 and 1,310 cm^{-1} may be attributed to the ν(C–O–C) vibration [10], and this vibration became apparently after modifying by the Mn(II). The absorbance spectrum at 1,561.78 cm^{-1} in LAC and 1,572.84 cm^{-1} in LAC-Mn were assigned to C=O in the quinine structure [11]. Compared the two infrared spectrum curves, the curve of LAC-Mn became sharp and strong, which indicated that Mn was adhered to LAC. more number of peaks appear in LAC-Mn

Fig. 4(b) and (c) showed the infrared spectrum curves of the two adsorbents and BF-load adsorbents. It can be seen that some new peaks emerged between 1,043 and 1,600 cm^{-1} and the curves became weaker. The range of 1,043.50–1,362.57 cm^{-1} may be the characteristic peaks of C–N stretching vibration, which indicated that BF was appeared on the surface of LAC and LAC-Mn. Furthermore, the LAC-BF had a high number peaks than the LAC-Mn-BF, indicating that the loading of Mn(II) changed the adsorption of BF onto LAC-Mn.

3.2. Effects of adsorbent dosage

The effect of adsorbent dosage for BF adsorption on LAC and LAC-Mn was discussed on the condition of various adsorbent dosages (0.1, 0.2, 0.4, 0.8, 1.0, 1.2, 1.6, 2.0, 2.4, and 3 g/L) at the BF concentration of 150 mg/L. It is shown in Fig. 5 that the removal efficiency escalated with the increasing of dosage, which can be explained that the doses increased effective

Table 1
The surface areas and porosities of LAC and LAC-Mn

Activated carbon	S_{BET} (m^2/g)	S_{ext} (m^2/g)	(%)	S_{mic} (m^2/g)	(%)	V_t (cm^3/g)	V_{mic} (cm^3/g)	(%)	D_p (nm)
LAC	509.46	242.38	47.58	267.08	52.42	0.310	0.124	40.00	1.29
LAC-Mn	582.50	214.79	36.87	367.71	63.13	0.408	0.182	44.61	1.23

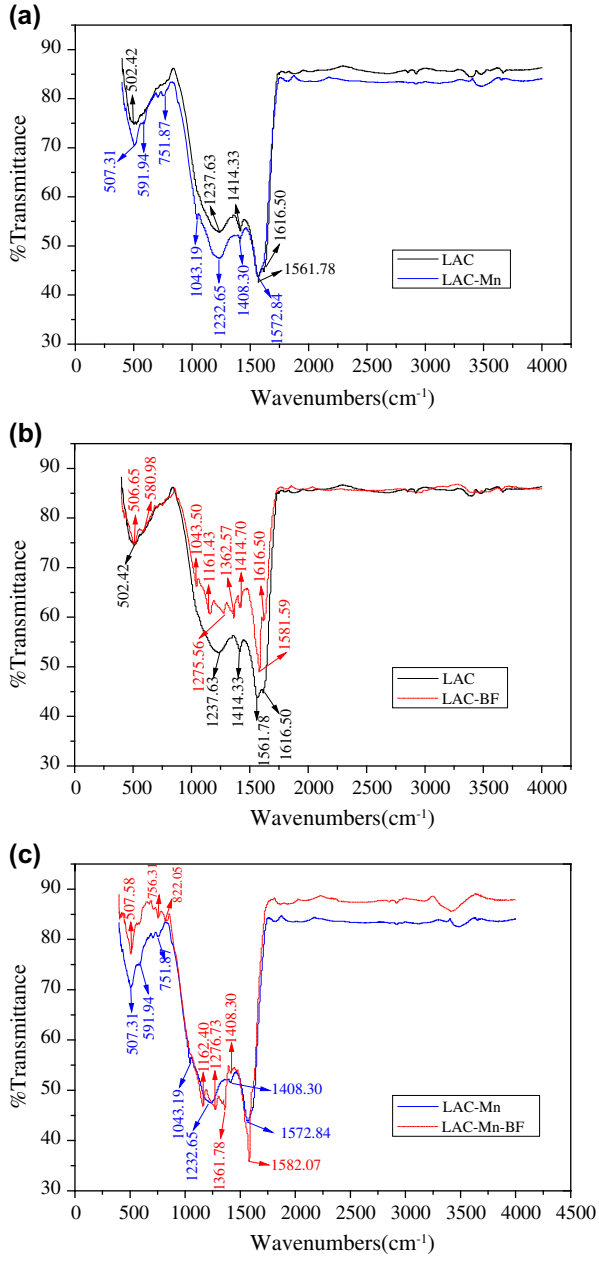

Fig. 4. FTIR spectra of the three adsorbents before and after BF adsorption.

surface area and thus added the adsorption sites effectively. Moreover, when the adsorbent dosage of LAC-Mn was more than 1 g/L, the dye removal percentage exceeded 90%; consequently, 1 g/L was identified as the optimum adsorbent dosage for subsequent experiments.

Compared with LAC, LAC-Mn had a better adsorption property, which showed that Mn(II) improved the adsorption capacity onto LAC-Mn. It can be explained that Mn(II) played a catalytic role in

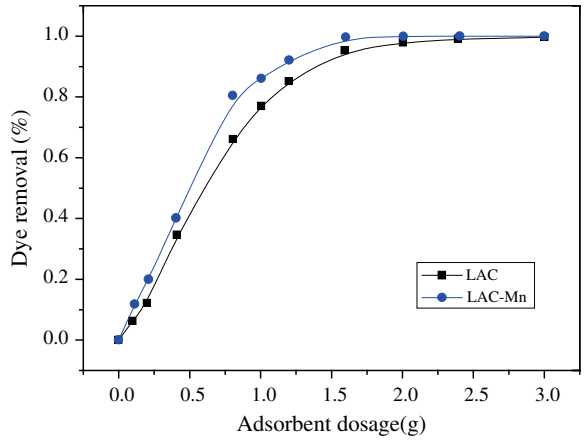

Fig. 5. The effect of adsorbents dosage on the removal of BF (C_0 = 150.0 mg/L, dosage = 0.1, 0.2, 0.4, 0.8, 1.0, 1.2, 1.6, 2.0, 2.4, 3 g/L, T = 20 ℃).

adsorbing BF, which reduced the activation energy under the same adsorbent dosage. Thus, the adsorption capacities enhanced. In addition, Mn-loaded would alter and introduce types of functional groups, which was also in favor of providing adsorption sites. Consequently, the effect of BF adsorption was elevated.

3.3. Effects of contact time

The effect of contact time to BF adsorption on LAC/LAC-Mn is shown in Fig. 6(a). It can be known that the adsorption capacity of BF increased rapidly at the beginning of 100 min, and then this trend slowed to equilibrium. It can be explained that a large number of idle adsorption sites were gradually occupied by the BF molecule. And more than 80% of this process was accomplished during the first 100 min. Fig. 6 (a) also shows that the equilibrium time for the two adsorbents was about 550 min, and the adsorption efficiency of BF onto LAC-Mn was better than LAC. Ultimately, 600 min was chosen as the shaking time for the further experiment.

3.4. Effect of pH and adsorption mechanism

The value of pH is one of the significant factors in the process of adsorption; it can alter the surface charge of adsorbent and species of BF. Fig. 7 displays the effect of initial solution on adsorption capacity. It indicates that BF was pH-dependent, namely, the adsorption effect was better under alkaline condition (pH 7–10) than the acid condition (pH 3–6) for both of the adsorbents. Similar results had been reported by Gupta et al. [2].

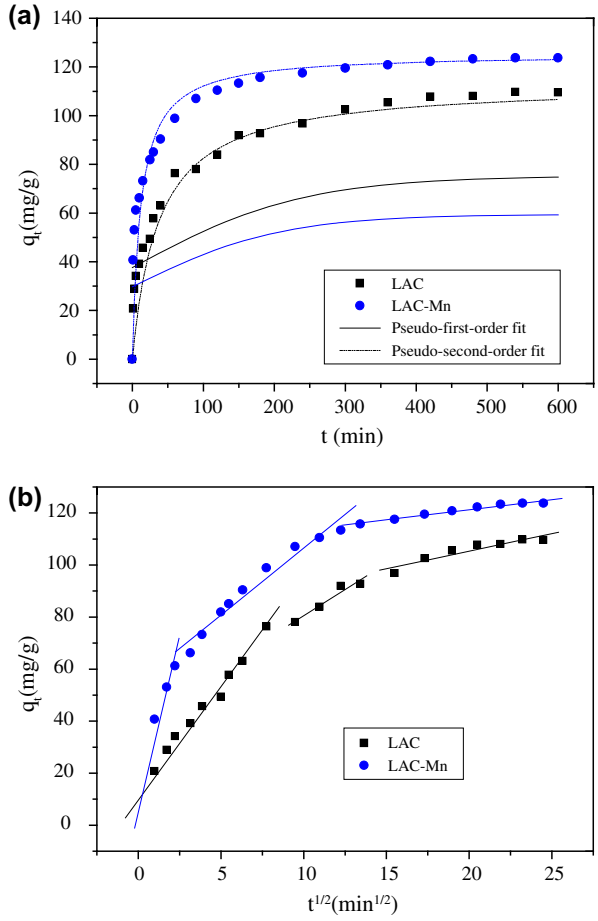

Fig. 6. (a) Adsorption kinetics of BF onto LAC and LAC-Mn, and modeling using the pseudo-first-order (dashed lines) and pseudo-second-order (solid lines) equations and (b) using intra-particle diffusion model.

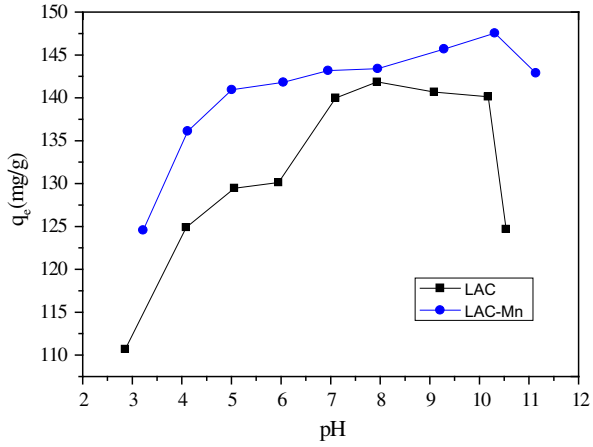

Fig. 7. The effect of pH on the adsorption amounts of BF (C_0 = 150.0 mg/L, dosage = 1.0 g/L, T = 20 ℃).

As seen from Fig. 7, when the value of pH increased from 3 to 8, the adsorption capacity of BF increased. BF molecules were protonated in acid condition and have positively charged surface, thus the cationic BF was the dominating forms in solution at acidic condition. Thus, ion exchange may be a considerable mechanism in adsorbing BF on LAC and LAC-Mn. The protons on the surface of LAC and LAC-Mn exchanged with cationic BF by positively charged groups [12], which made BF molecules connected to adsorbents. Consequently, a part of protons entered into the solutions. Furthermore, the structure of BF would be destroyed at acidic condition. In basic condition, the surface of LAC and BF molecules embodied a negative charge, indicating that the interaction would become inferior owing to electrostatic repulsions. For LAC-Mn, the Mn(II) in alkaline region can combine with part of the OH^- and decrease the assault of OH^-. Hence, the adsorption capacity still enhanced. But the adsorption capacity increased; there might be other mechanisms to enhance it. The molecule of basic fuchsin contains three $-NH_2$ and three benzene ring structures, in which benzene ring structure is the chromogenic functional group and $-NH_2$ is the auxochromic functional group. The conjugated system in BF increased the mobility of the electrons, which made binding force of π electrons weak, and thus the energy required for $\pi \rightarrow \pi^*$ dropped. The activated carbon also contains basic π-band of the graphitic planes [13]. Thus, the π-electron-donor–acceptor (EDA) interaction [14] may participate in the BF adsorption onto LAC or LAC-Mn. The leather material contains protein composition, therefore, has a strong hydrophobicity, which can integrate with hydrophobic substances.

Fig. 8 shows the XPS survey spectra for LAC-Mn before and after BF adsorption. It is indicated that elements C and O emerged on the LAC-Mn and LAC-Mn-BF. The XPS spectra of Mn $2p_{3/2}$ shows intensive peaks at 645.388 and 641.601 eV for LAC-Mn shift slightly to 642.349 and 640.972 eV after adsorb BF. It could be explained that the Mn(IV) oxidized into Mn(II), and BF was deoxidated, thus the color faded. Consequently, ion exchange, π-EDA interaction, and hydrophobicity are the mechanism of adsorbing BF by LAC and LAC-Mn.

3.5. Adsorption kinetics

The adsorption kinetics model is an important tool to discuss the adsorption process and adsorption mechanism. The experimental date obtained were simulated using pseudo-first-order Eq. (5), pseudo-second-order Eq. (6), and intraparticle diffusion models Eq. (7) [15,16].

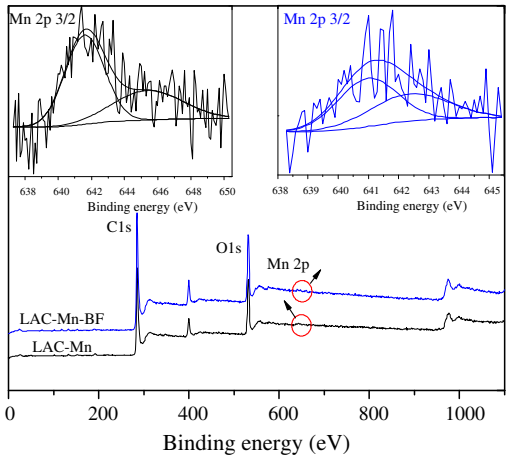

Fig. 8. XPS survey spectra for LAC-Mn before and after BF adsorption.

$$\ln(q_e - q_t) = \ln q_t - k_1 t \tag{5}$$

$$\frac{t}{q_t} = \frac{1}{k_2 q_e^2} + \frac{1}{q_e} t \tag{6}$$

$$q_t = k_{int} t^{1/2} + C_i \tag{7}$$

where q_e and q_t (mg/g) are the amounts of BF adsorbed at equilibrium and at time t (min), respectively; k_1 (min^{-1}), k_2 (g/(mg.min)), and k_{int} (mg/g $min^{1/2}$) are the pseudo-first-order rate constant, pseudo-second-order rate constant, and the intra-particle diffusion rate constant, separately; C_i represents the thickness of boundary layer. And according to known dates, k_1, k_2, k_{int}, and C_i can be obtained by drawing fitted cure.

Table 2 shows kinetic model parameters and coefficients for basic fuchsin adsorption. It is revealed that the pseudo-second-order kinetic model was more appropriate to describe this adsorption process than the pseudo-first-order kinetic model due to the high correlation coefficients. Moreover, the adsorption capacity ($q_{e,cal}$) from pseudo-second-order kinetic model was more closer to experimental data ($q_{e,exp}$). Fig. 7(a) displays the adsorption kinetics and modeling of LAC and LAC-Mn using the pseudo-first-order and pseudo-second-order models, which also illustrated this point.

The intra-particle diffusion is a model of rate-limiting step, which is determined by the plot of q_t versus $t^{1/2}$. It is revealed in Fig. 7(b) that the lines are multilinearity and do not pass through the origin, indicating several steps occurred in the process of adsorbing BF onto the two adsorbents. There were three stages for the adsorption of BF onto LAC and LAC-Mn. At the beginning stage, the sharp phase was the result of external diffusion of BF molecules, namely the film diffusion. The second phase was the rate-limiting (pore diffusion or intraparticle diffusion) which was gradually adsorbed to the adsorbents, the third stage finally slowed down to equilibrium due to the low concentrate of BF and aperture saturated of activated carbons. Table 3 shows the intra-particle diffusion model parameters for the adsorption of BF onto LAC and LAC-Mn, the increasing C_i indicates an increasing of the thickness of the boundary layer.

3.6. Adsorption isotherms and thermodynamics

3.6.1. Adsorption isotherms

Adsorption isotherm is often used to reflect the adsorbate distribution between the liquid and solid. In this study, the experiment was conducted at different temperature (20, 30, and 40 °C), and the obtained data were fitted using three commonly used models, namely Langmuir, Freundlich, and Tempkin isotherms [17]. The equations are as follows:

$$\frac{C_e}{q_e} = \frac{1}{q_m K_L} + \frac{C_e}{q_m} \tag{8}$$

$$\ln q_e = \ln K_F + \frac{1}{n} \ln C_e \tag{9}$$

$$q_e = B_T \ln A_T + B_T \ln C_e \tag{10}$$

where C_e (mg/g) is the equilibrium concentration of basic fuchsin, q_e (mg/g) is the amounts of BF adsorbed at equilibrium, and q_m (mg/g) is the maximum adsorption capacity. K_L (L/mg) is the Langmuir adsorption constant, K_F ((mg/g) $(L/mg)^{1/n}$) is the Freundlich constant related to adsorption capacity, n is the Freundlich exponent which represents adsorption intensity, B_T is the Tempkin constant, and A_T (L/min) is the equilibrium binding constant.

The fitting curves for the two adsorbents were drawn and the parameters can be acquired and shown in Table 4. It displayed that Langmuir model had a correlation coefficient (R^2) of more than 0.99, which indicated that Langmuir model is more suitable to describe this adsorption process than the other two equations. Thus, the adsorption of BF onto the two adsorbents inclined to be monolayer adsorption. The maximum adsorption amounts of LAC and LAC-Mn reached to 139.28 and 182.48 mg/L at 40 °C, q_m and K_F enhanced with the increase of temperature, which proved this adsorption was an endothermic process.

Table 2
Kinetics parameters for basic fuchsin adsorption onto LAC and LAC-Mn

Activated carbon	$q_{e,exp}$ (mg/g)	Pseudo-first-order kinetic model			Pseudo-second-order kinetic model		
		$k_1 \times 10^{-3}$ (min^{-1})	$q_{e,cal}$ (mg/g)	R^2	$k_2 \times 10^{-4}$ (g/mg min)	$q_{e,cal}$ (mg/g)	R^2
LAC	109.55	8.35	75.24	0.983	2.36	113.25	0.997
LAC-Mn	123.73	9.56	59.47	0.957	6.73	125.47	0.999

Table 3
Intra-particle diffusion model parameters for the adsorption of BF onto LAC and LAC-Mn

Activated carbon	The first stage			The second stage			The third stage		
	k_{int1} (mg/g $min^{1/2}$)	C_1	R^2	k_{int2} (mg/g $min^{1/2}$)	C_2	R^2	k_{int3} (mg/g $min^{1/2}$)	C_3	R^2
LAC	8.73	9.58	0.962	4.01	40.38	0.943	1.35	78.29	0.880
LAC-Mn	27.19	4.95	0.946	5.15	55.02	0.959	0.77	105.84	0.966

Moreover, the values of n were higher for LAC-Mn than LAC, indicating the LAC-Mn was more favorable than LAC. It can be shown that the load of Mn^{2+} improved the properties of LAC significantly. A comparison of the adsorption capacities for basic fuschin by other low-cost adsorbents is displayed in Table 5. It is shown that leather waste is a promising precursor for preparing activated carbon.

3.6.2. Adsorption thermodynamics

Adsorption thermodynamics parameters, enthalpy change (ΔH), Gibbs free energy change (ΔG), and entropy change (ΔS) were calculated by the following equations [18,19]:

$$\Delta G = -RT \ln K \quad (11)$$

$$\Delta G = \Delta H - T\Delta S \quad (12)$$

where R (8.314 J/(mol·K)) is the universal gas constant, T (K) is the absolute temperature, and K (L/mol) is the Langmuir constant. ΔH and ΔS were obtained from the intercept and slope of the plot of ΔG versus T.

It can be known from Table 6 that the adsorption process is spontaneous due to the negative ΔG values. And the positive ΔH values for the two adsorbents indicated an endothermic process, which was consistent with the previous mentioned. The values of ΔH are in the range of 2.1–20.9 kJ/mol, which belong to physical adsorption [20]. The positive values of ΔS reflect that the appetency between the adsorbents and basic fuchsin becomes random.

3.7. Desorption studies

Desorption experiments can be used to further determine the adsorption mechanism of the adsorption process as well as the feasibility of activated

Table 4
Isotherm model constants for BF adsorption onto adsorbents

Isotherm models	Constants	LAC			LAC-Mn		
		20℃	30℃	40℃	20℃	30℃	40℃
Langmuir	q_m (mg/g)	132.28	135.14	139.28	130.38	160.51	182.48
	k_L (L mg^{-1})	0.47	0.72	0.70	0.68	3.30	1.05
	R^2	0.998	0.996	0.997	0.991	0.999	0.998
Freundlich	k_F (mg g^{-1})(l/mg)$^{1/n}$	71.86	77.55	80.45	101.39	107.61	111.97
	n	7.61	8.09	8.19	13.16	10.03	8.44
	R^2	0.957	0.926	0.958	0.744	0.966	0.993
Tempkin	B_T	13.63	13.05	12.95	8.62	12.22	15.39
	A_T	145.18	329.31	475.33	160,331.69	8,561.24	1,881.83
	R^2	0.989	0.973	0.984	0.719	0.973	0.997

Table 5
Comparison of the adsorption capacity with literature data

Adsorbent	q_m (mg/g)	Data resource
Cation-exchange resin	178.6	[21]
Graphene-based magnetic nanocomposite	89.4	[22]
Super absorbent polymer	11.7	[23]
Bottom ash	9	[2]
Deoiled soya	13	[2]
AC/ferrospinel composite	101.0	[24]
LAC	139.28	In our study
LAC-Mn	182.48	In our study

Table 6
Thermodynamic parameters for the adsorption of basic fuchsin onto two adsorbents

Activated carbon	t (℃)	ΔG (kJ/mol)	ΔH (kJ/mol)	ΔS (kJ/(mol K))
LAC	20	−29.151	15.097	0.151
	30	−31.260		
	40	−32.185		
LAC-Mn	20	−30.064	15.390	0.159
	30	−35.074		
	40	−33.245		

carbon regeneration. Little desorption (<0.7%) with different concentrates of NaOH solutions, indicated that BF was adsorbed onto activated carbons mainly by chemisorption, and the strong affinity between BF and adsorbents may be electrostatic attraction or ion exchange. Thus, desorption of BF was difficult to achieve.

4. Conclusions

In this study, leather waste was chosen as the precursor to prepare activated carbon, and then was modified by Mn(II). The basic fuchsin adsorption capacity improved from 139.28 to 182.48 mg/g (∼31%) by loading Mn onto LAC. And the BF adsorption indicated a pH-dependant behavior for the two adsorbents. The mechanisms for basic fuchsin adsorption were likely cation exchange, hydrophobicity and, π-EDA interaction. The data fit the pseudo-second-order kinetics model better than the pseudo-first-order kinetics, while the Langmuir isotherm equation can describe the adsorption isotherms. Thus, it was displayed that the BF adsorption was a process of chemisorption and monolayer adsorption. Thermodynamics results showed that the adsorption processes was a spontaneous and endothermic process. The present work showed LAC is a promising adsorbent and would promote the development of dye adsorption.

Acknowledgments

The authors would like to acknowledge financial support for this work provided by Shandong province Postdoctoral fund.

References

[1] S. Wang, H. Li, Dye adsorption on unburned carbon: Kinetics and equilibrium, J. Hazard. Mater. 126 (2005) 71–77.
[2] V.K. Gupta, A. Mittal, V. Gajbe, J. Mittal, Adsorption of basic fuchsin using waste materials—bottom ash and deoiled soya—as adsorbents, J. Colloid Interface Sci. 319 (2008) 30–39.
[3] M. Belhachemi, Z. Belala, D. Lahcene, F. Addoun, Adsorption of phenol and dye from aqueous solution using chemically modified date pits activated carbons, Desalin. Water Treat. 7 (2009) 182–190.
[4] M.A.M. Salleh, D.K. Mahmoud, W.A.W.A. Karim, A. Idris, Cationic and anionic dye adsorption by agricultural solid wastes: A comprehensive review, Desalination 280 (2011) 1–13.
[5] K.S. Thangamani, M. Sathishkumar, Y. Sameena, N. Vennilamani, K. Kadirvelu, S. Pattabhi, S.E. Yun, Utilization of modified silk cotton hull waste as an adsorbent for the removal of textile dye (reactive blue MR) from aqueous solution, Bioresour. Technol. 98 (2007) 1265–1269.
[6] V.K. Garg, M. Amita, R. Kumar, R. Gupta, Basic dye (methylene blue) removal from simulated wastewater by adsorption using Indian Rosewood sawdust: A timber industry waste, Dyes Pigm. 63 (2004) 243–250.
[7] M.M. Abd El-Latifa, A.M. Ibrahim, Removal of reactive dye from aqueous solutions by adsorption onto activated carbons prepared from oak sawdust, Desalin. Water Treat. 20 (2010) 102–113.
[8] I.C. Kantarli, J. Yanik, Activated carbon from leather shaving wastes and its application in removal of toxic materials, J. Hazard. Mater. 179 (2010) 348–356.
[9] H. Liu, X. Wang, G. Zhai, J. Zhang, C. Zhang, N. Bao, C. Cheng, Preparation of activated carbon from lotus stalks with the mixture of phosphoric acid and pentaerythritol impregnation and its application for Ni(II) sorption, Chem. Eng. J. 209 (2012) 155–162.
[10] J. Jaramillo, P.M. Álvarez, V. Gómez-Serrano, Oxidation of activated carbon by dry and wet methods: Surface chemistry and textural modifications, Fuel Process. Technol. 91 (2010) 1768–1775.
[11] W.T. Tsai, C.Y. Chang, M.C. Lin, S.F. Chien, H.F. Sun, M.F. Hsieh, Adsorption of acid dye onto activated carbons prepared from agricultural waste bagasse by ZnCl2 activation, Chemosphere 45 (2001) 51–58.
[12] W. Liu, J. Zhang, C. Zhang, L. Ren, Sorption of norfloxacin by lotus stalk-based activated carbon and iron-doped activated alumina: Mechanisms, isotherms and kinetics, Chem. Eng. J. 171 (2011) 431–438.
[13] W. Nakbanpote, P. Thiravetyan, C. Kalambaheti, Preconcentration of gold by rice husk ash, Miner. Eng. 13 (2000) 391–400.
[14] E.D. Lavrinenko-Ometsinskaya, K.A. Kazdobin, V.V. Strelko, Quantum-chemical evaluation of electron-donor properties of ordinary and modified carbon sorbents, Theor. Exp. Chem. 25 (1989) 666–670.

[15] P. Janoš, P. Michálek, L. Turek, Sorption of ionic dyes onto untreated low-rank coal—oxihumolite: A kinetic study, Dyes Pigm. 74 (2007) 363–370.
[16] I.A.W. Tan, A.L. Ahmad, B.H. Hameed, Adsorption of basic dye on high-surface-area activated carbon prepared from coconut husk: Equilibrium, kinetic and thermodynamic studies, J. Hazard. Mater. 154 (2008) 337–346.
[17] M.M. Abd El- Latif, A.M. Ibrahim, Adsorption, kinetic and equilibrium studies on removal of basic dye from aqueous solutions using hydrolyzed Oak sawdust, Desalin. Water Treat. 6 (2009) 252–268.
[18] N.K. Amin, Removal of direct blue-106 dye from aqueous solution using new activated carbons developed from pomegranate peel: Adsorption equilibrium and kinetics, J. Hazard. Mater. 165 (2009) 52–62.
[19] P. Wang, R. Zhang, C. Hua, Removal of chromium (VI) from aqueous solutions using activated carbon prepared from crofton weed, Desalin. Water Treat. 51 (2012) 2327–2335.
[20] R.I. Yousef, B. El-Eswed, A.a.H. Al-Muhtaseb, Adsorption characteristics of natural zeolites as solid adsorbents for phenol removal from aqueous solutions: Kinetics, mechanism, and thermodynamics studies, Chem. Eng. J. 171 (2011) 1143–1149.
[21] G. Bayramoglu, B. Altintas, M.Y. Arica, Adsorption kinetics and thermodynamic parameters of cationic dyes from aqueous solutions by using a new strong cation-exchange resin, Chem. Eng. J. 152 (2009) 339–346.
[22] C. Wang, C. Feng, Y. Gao, X. Ma, Q. Wu, Z. Wang, Preparation of a graphene-based magnetic nanocomposite for the removal of an organic dye from aqueous solution, Chem. Eng. J. 173 (2011) 92–97.
[23] R. Dhodapkar, N.N. Rao, S.P. Pande, T. Nandy, S. Devotta, Adsorption of cationic dyes on Jalshakti®, super absorbent polymer and photocatalytic regeneration of the adsorbent, React. Funct. Polym. 67 (2007) 540–548.
[24] L. Ai, J. Jiang, Fast removal of organic dyes from aqueous solutions by AC/ferrospinel composite, Desalination 262 (2010) 134–140.